Journal of Magnetism and Magnetic Materials 550 (2022) 169053

Contents lists available at ScienceDirect

Journal of Magnetism and Magnetic Materials

journal homepage: www.elsevier.com/locate/jmmm

Research articles

Influence of polymorphic magnetic phases on exchange bias effect in bulk and nanocrystalline $La_{0.375}Ca_{0.625}MnO_3$ compound

Soma Chatterjee [a], Kalipada Das [b,*], I. Das [a]

[a] CMP Division, Saha Institute of Nuclear Physics, HBNI, AF-Bidhannagar, Kolakta 700064, India
[b] Department of physics, Seth Anandram Jaipuria College, 10-Raja Nabakrishna Street, Kolkata 700005, India

ARTICLE INFO

Keywords:
Manganites
Exchange bias effect
Nanocrystalline

ABSTRACT

Magnetic properties and exchange bias effect of the polycrystalline and nanocrystalline $La_{0.375}Ca_{0.625}MnO_3$ compounds have been presented. With reduction of the particle size, uncompensated surface spin induced ferromagnetism is pronounced in nanocrystalline sample. However, at higher magnetic field value, long range charge ordering (associated with antiferromagnetic nature) is predominant even in nanoparticles similar as bulk counterpart. Exchange bias properties of both compounds have been found at low temperature with increasing nature depending on the cooling magnetic field. Significantly large value of the exchange bias effect in this particular bulk compound and modification of it in nanocrystalline sample is addressed considering the disordered polymorphs developed within the charge-orbital ordered phase.

1. Introduction:

The physical properties of doped perovskite manganite with general formula $R_{1-x}B_xMnO_3$ (R is trivalent rare-earth ion, B is bivalent ion) were extensively studied during the last two decades [1–6]. Generally, undoped perovskite manganite ($RMnO_3$) exhibits antiferromagnetic ground state. In case of doped manganite several important properties (such as large magnetocaloric effect (MCE), colossal magnetoresistance effect (CMR), metal–insulator transition, Phase separation, etc.) were observed due to the presence of Mn^{4+} ions [3,4]. Exchange Bias (EB) phenomena is also observed in doped perovskite manganites [5,6]. EB is associated with the systems containing the competing nature between the ferromagnetic and antiferromagnetic interfaces. Such exchange coupling produced the unidirectional pinning of interfacial spins around the magnetic phase boundary. Generally, zero field cooled M-H loops are symmetric in nature. However, for some materials, asymmetric M-H loops (shifting of the loop towards the negative fields and positive magnetizations) have been observed when the sample is cooled down in the presence of magnetic field and originates the exchange bias phenomena. Except this fact, the several diverse nature regarding the origin of exchange bias phenomena is discussed in the previously reported articles [7–16]. The comprehensive study revealed the existence of disordered interfacial spins as "spin clusters" analogous to a spin glass at the interface between the FM and AFM layers [7]. Additionally, the nature of the coupling of the interfacial spins may also be responsible for the exchange bias phenomena [8]. Ali et al. have given an elegant demonstration of how EB is observed in Co/CuMn thin film interfaces formed between conventional ferromagnets (FM) and spin glasses (SG) [9]. These studies pinpoint an important fact that the presence of an FM-AFM interface is not a necessary condition to induce EB in all cases. EB phenomena is also observed in various types of interfaces, such as ferromagnet/ferrimagnet, soft ferromagnet/hard ferromagnet, ferrimagnet/antiferromagnet, ferrimagnet/ferrimagnet (FI/FI), antiferromagnet/diluted ferromagnetic semiconductor (AFM/DMS) etc. [10–16]. Among the manganite families, significantly large exchange bias effect was reported for $Sm_{1-x}Ca_xMnO_3$ system by several groups [17]. According to the reported studies, EB effect is closely related with the charge ordering phenomena which is almost a generic property of nearly half doped samples [17]. Charge ordering appears below a certain temperature called charge order transition temperature (T_{CO}). Charge ordering is the real space ordering between Mn^{3+} and Mn^{4+} ions that observed nearly half-doped manganite compounds. $La_{1-x}Ca_xMnO_3$ is one of the most well-studied compounds among the perovskite manganite that possess many fascinating physical properties [18–21]. Depending on the doping concentration x, complete phase diagram of $La_{1-x}Ca_xMnO_3$ compound was already reported [22,23]. According to the phase diagram, charge ordering is observed for $x > 0.5$ of the compounds. The influence of charge order state with the external magnetic field was already reported for several manganites [24,25].

In this work we have studied the magnetic properties of bulk as well as nanoparticles of $La_{1-x}Ca_xMnO_3$ with $x = 0.625$. Bulk $La_{0.375}Ca_{0.625}$

* Corresponding author.
E-mail address: kalipadadasphysics@gmail.com (K. Das).

https://doi.org/10.1016/j.jmmm.2022.169053
Received 9 October 2021; Received in revised form 11 December 2021; Accepted 11 January 2022
Available online 22 January 2022

Table 1
Lattice parameters of LCMO-bulk and LCMO-nanocrystalline compounds.

Compound	Space group	a (Å)	b (Å)	c (Å)
LCMO-bulk	Pnma	5.6200	7.5236	5.8338
LCMO-nanocrystalline	Pnma	5.5590	7.4711	5.8087

MnO_3 compound exhibits long range charge ordering (irrespective of the external magnetic field). Previous study on this particular compound indicates about the special feathers regarding the magnetic ground state at the low temperature region [25]. The magnetic properties at low temperature are governed by the competing nature of the polymorphic disordered phase and long range ordered magnetic phase [25]. We have investigated the modification of the physical properties with increasing magnetic disorderness (nanoparticles). It is already reported that with increasing charge order stability (large value of T_{CO}), Exchange bias is also increasing [17].

Our present experimental findings indicate that higher value of exchange bias is also influenced by not only the charge-ordering stability but also the magnetic structural transition of the compound. Generally, due to the reduction of the particle size of the manganite compounds, long range nature of the magnetic interaction is quietly suppressed [26,27]. Core–shell model suggest that when charge ordered antiferromagnetic (CO-AFM) bulk compound is transformed into nanoparticles then a ferromagnetic (FM) shell is appeared outside the antiferromagnetic (AFM) core [28,29]. In our study, prominent ferromagnetism is appeared for H = 500 Oe external magnetic field. However, CO signature becomes pronounced for higher magnetic field values. Here the magnetic study reveals that exchange bias phenomena exist for both bulk (with significantly large value) and nanocrystalline samples. The quantitative value of exchange bias field for this particular doping concentration is larger than any other doping of LCMO compound [30,31]. Such anomalous exchange bias effect was addressed by considering the coexisting nature of the pnma (disorder) - pnma (order) magnetic phases at low temperature region.

2. Sample preparation, characterizations and measurements

The $La_{0.375}Ca_{0.625}MnO_3$ compounds are prepared by the conventional sol–gel method. Pure La_2O_3, $CaCO_3$, and MnO_2 are used as starting elements. At first, high pure (99.99%) rare-earth oxide was preheated at 500 °C. Required amount of all the primary elements are converted into their nitrate forms by using suitable amount of nitric acid and millipore water. Except MnO_2 all the individual components give a clear solution. When required amount of oxalic acid is added with the MnO_2 solution, after 5–6 h a clear solution is reached. Then all the individual clear solution is mixed up by a magnetic stirrer and suitable amount of citric acid was added with it. The mixed solution was evaporated at 80–90 °C by using a water bath to product the gel. It was decomposed at higher temperature and black porous powder was formed. Finally, palletized powder was annealed at 1400 °C (36 h duration) for the preparation of bulk compound and 1000 °C for (6 h) for nanocrystalline compound.

Room temperature powder X-ray diffraction study was carried out by Rigaku TTRAX-III diffractometer using Cu-K_α radiation(λ = 1.54 Å). A field emission Scanning electron microscope (FESEM) was used to study the grain size and the surface morphology of the nanoparticles. Energy Dispersive X-ray analysis (EDAX) was done for compositional analysis of the compound. Magnetic measurements were performed by Super Conducting Quantum Interference Device (SQUID-VSM) magnetometer.

3. Results and discussion

Room temperature X-ray diffraction data confirms about the single-phase nature of both polycrystalline and nanocrystalline $La_{0.375}Ca_{0.625}MnO_3$ compound. Rietveld profile fitting of the X-ray diffraction data (by considering 'pnma' space group symmetry) for bulk and nanoparticles are shown in Fig. 1(a) and (b) respectively. The extracted lattice parameter for both compounds are shown in Table 1.

The scanning electron microscopy (SEM) images for bulk and nanoparticles are shown in Fig. 1(c) and (d) respectively. The SEM image reveals that the average particle size for nanoparticles is ~200 nm.

Temperature dependent magnetization [M(T)], for both the samples were measured (from 5 K to 350 K) in three different protocols: Zero field cooled warming (ZFCW), Field cooled cooling (FCC) and Field cooled warming (FCW) which are shown in Fig. 2.

In the presence of small magnetic field, charge ordered antiferromagnetic nature of the bulk sample is clearly visible (Fig. 2(a)). However, ferromagnetic nature is pronounced in case of nanocrystalline sample (Fig. 2(b)). Fig. 2(c), (d) represents the temperature dependent of magnetization at 70 kOe external magnetic field. The bulk counterpart exhibits antiferromagnetic transition at 115 K and charge-ordering near about 250 K. Charge-ordering transition remains at the same temperature even for 70 kOe external magnetic field value. It is well studied that AFM bulk counterpart transformed into the core–shell type structure in its nanoparticle formation (AFM core within FM shell). As a result, we have observed the FM nature for the ground state of nanoparticles (at H = 500 Oe) (shown in Fig. 2(b)). Inset of the (Fig. 2) shows the variation of inverse susceptibility with temperature (from FCW data of the magnetization) along with Curie–Weiss fitting (using-Eq. (1)) at the higher temperature.

$$\chi = \frac{C}{T-\theta} \tag{1}$$

Positive values of θ support the existence of ferromagnetic interaction at low temperature for all the samples. Experimental curves indicate linear nature above $T \sim 290$ K. It is also interesting to note that a typical nature of Griffith phase (GP)(presence of ferromagnetic cluster within a paramagnetic matrix below 290 K) is observed in nearest compounds (x = 0.50, $x = 0.67$, $x = 0.75$) by the downturn nature of the inverse susceptibility before reaching the curie temperature [30,32–34]. However, for this particular compound $x = 0.625$ signature of GP is not observed.

Magnetization as a function of external magnetic field for polycrystalline bulk and nanoparticles (at some different constant temperature) are shown in Fig. 3(a) and (b) respectively. In Fig. 3(a), only straight line like response is observed which corresponds to the charge ordered antiferromagnetic like nature of the bulk counterpart. Whereas for nanocrystalline compound low temperature isotherms show the hysteresis loop (which corresponds to ferromagnetic like behavior) and for high temperature it will become straight line (corresponds to paramagnetic) (shown in Fig. 3(b)).

At low temperature region ferromagnetic and antiferromagnetic phase coexist for bulk as well as nanoparticles of $La_{0.375}Ca_{0.625}MnO_3$ compound, so we can expect exchange bias for both the samples. If H_1 and H_2 denote the left and right coercivity fields respectively then exchange bias field is defined by $H_{EB} = (H_1 + H_2)/2$ and coercivity field is $H_{CO} = (H_1 - H_2)/2$. Isothermal magnetization measurements under FC protocol (at 5 K under different cooling fields) was carried out to check the exchange bias phenomena of these compounds. Isothermal magnetic measurement at $T = 5$ K after cooling down the sample in the presence of magnetic field exhibits pronounced exchange bias effect. In our studied sample, existence of ferromagnetic and antiferromagnetic interfaces played the primary role. In addition to that, competing nature of different magnetic domains (ordered/disordered phase) and short range correlation between uncompensated surface

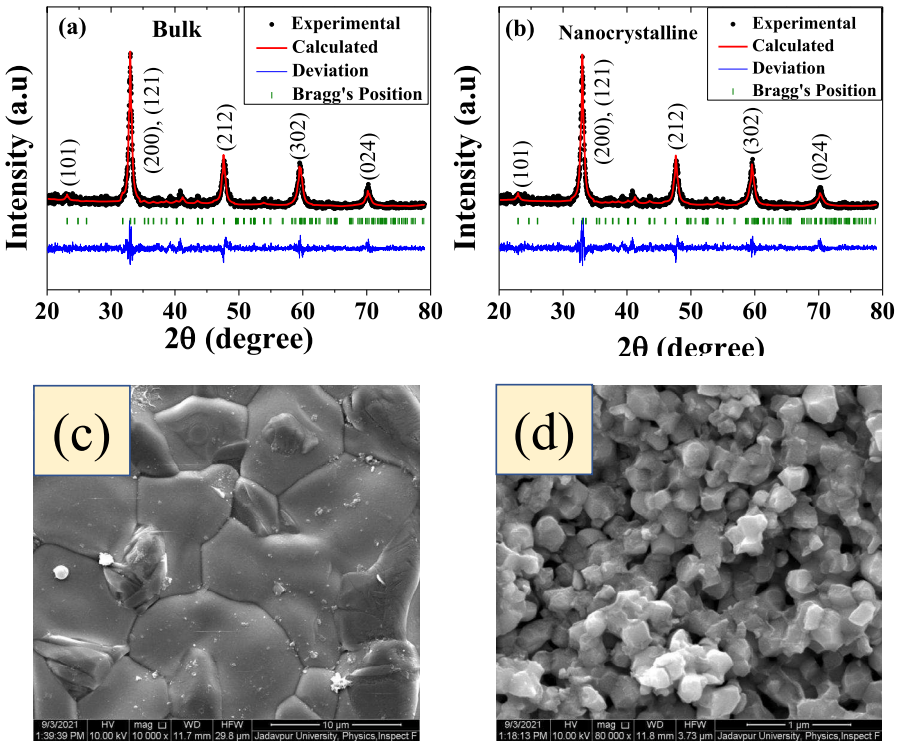

Fig. 1. Room temperature X-ray diffraction pattern (along with profile fitting) for (a) bulk and (b) nanocrystalline compound. (c) and (d) represents the scanning electron microscopy images of bulk and nanocrystalline compound respectively.

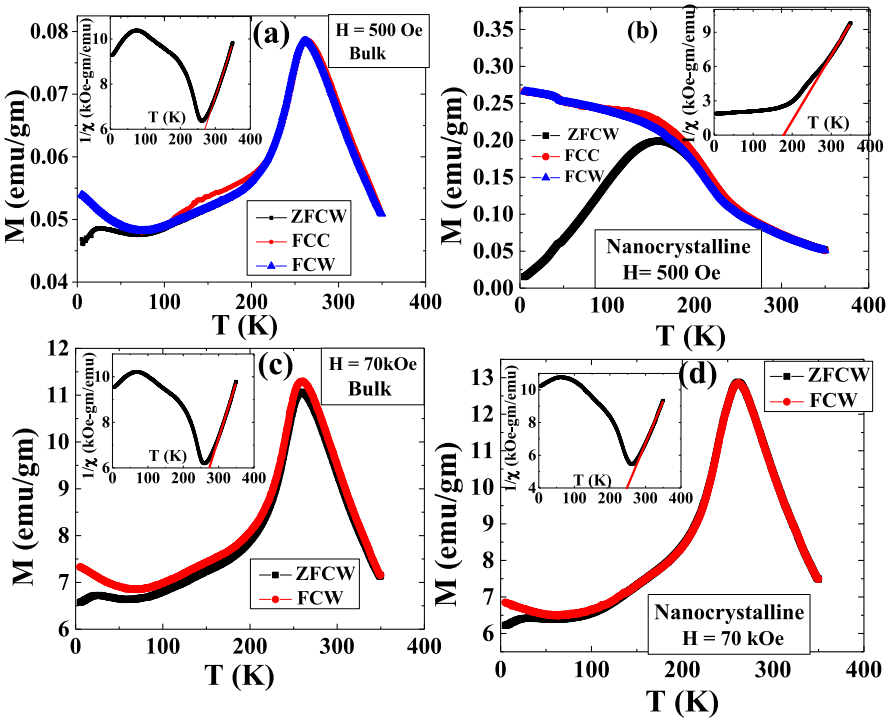

Fig. 2. Temperature dependence of ZFCW, FCW, FCC magnetization at H = 500 Oe (a) for bulk and (b) for nanocrystalline $La_{1-x}Ca_xMnO_3$ compound respectively. The nature of magnetization as a function of temperature at higher magnetic field is shown in (c) for bulk compound and (d) for nanocrystalline compound. Insets show temperature dependence of inverse susceptibility (calculated from FCW magnetization).

spins influenced the exchange bias phenomena in bulk and nanocrystalline compound. For the bulk counterpart, [Fig. 4(a)] EB phenomena is so large that both H_1 and H_2 are in the negative direction, while for nanocrystalline [Fig. 4(b)] H_1 is in the left and H_2 is in the right side. For the assurance of the EB effect M(H) measurement was done at T = 5 K for −70 kOe cooling field and the same shift in opposite

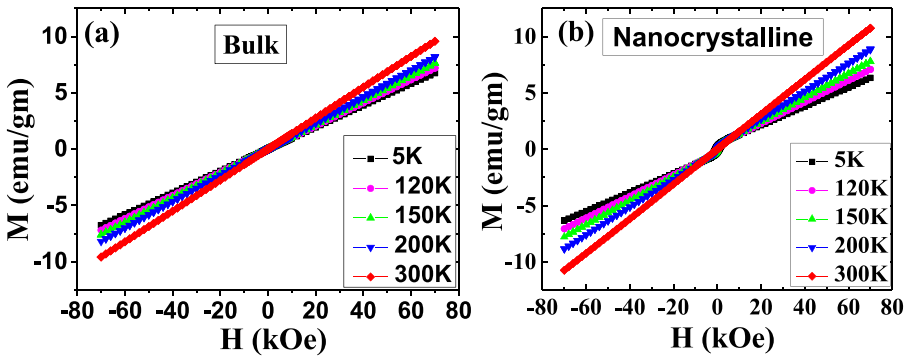

Fig. 3. (a) and (b) represents the magnetization as a function of external magnetic field at some selected temperature for bulk and nanocrystalline compound respectively.

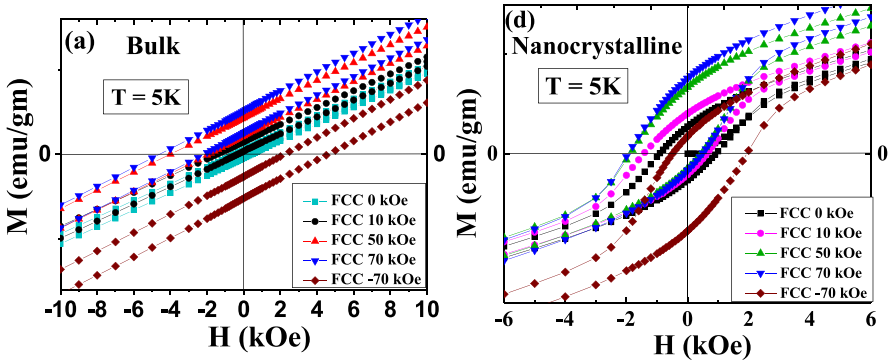

Fig. 4. (a) and (b) represents enlarged view of asymmetric hysteresis loop (exchange bias effect) at the low field region for several cooling fields.

Table 2
List of ΔH_1 and ΔH_2 for bulk and nanocrystalline compounds.

Cooling field (kOe)	ΔH_1 (bulk)	ΔH_1 (nano)	ΔH_2 (bulk)	ΔH_2 (nano)
10	−0.95	−0.494	−0.73	−0.268
50	−3.45	−0.934	−2.35	−0.468
70	−4.13	−1.01	−2.61	−0.42

direction was observed (compared to +70 kOe cooling field) for both the compounds.

We can also define $\Delta H_1 = H_1(FC) - H_1(ZFC)$ and $\Delta H_2 = H_2(FC) - H_2(ZFC)$ (where $H_1(FC)$, $H_2(FC)$ are left and right coercivities respectively in FC mode and $H_1(ZFC)$, $H_2(ZFC)$ are the same in ZFC mode. Here ΔH_1 and ΔH_2 indicates the strength of interfacial interaction between FM/AFM interfaces. At this interface, a unidirectional anisotropy is formed along the direction of the cooling field [35,36]. The value of ΔH_1 and ΔH_2 for bulk and nanoparticles at different cooling field are listed below (Table 2)

Exchange bias effect for the bulk counterpart of this compound (maximum 3.37 kOe at 70 kOe cooling field) is much larger than the nanoparticles (maximum 0.72 kOe at 70 kOe cooling field). Such value of EB field are large compared to the many others Ca doping concentration of $La_{1-x}Ca_xMnO_3$, $Sm_{1-x}Ca_xMnO_3$ and others manganite family also. Some manganite family with their EB field are shown in Table 3.

The reason of the higher value of exchange bias may be the 'pnma - pnma' structural transition along with the charge order stability. For some others compound with nearly same charge order stability, but exchange bias is not so large for them [30,31]. Such anomalous exchange bias effect in the studied compound may be understood as follows. $La_{0.375}Ca_{0.625}MnO_3$ compound shows pnma - pnma structural transition at low temperature region where a significant percentage of disordered polymorphic phase (pnma) coexist with the charge-orbital

Table 3
List of exchange bias field at T = 5 K for several manganite compounds. Cooling field was 50 kOe.

Compound (kOe)	Dimension	Exchange bias field (kOe)	Reference
$La_{0.45}Ca_{0.55}MnO_3$	bulk	0.05	[31]
$La_{0.40}Ca_{0.60}MnO_3$	bulk	2.25	[31]
$La_{0.35}Ca_{0.65}MnO_3$	bulk	1.77	[31]
$La_{0.30}Ca_{0.70}MnO_3$	bulk	1.07	[31]
$La_{0.25}Ca_{0.75}MnO_3$	bulk	0.39	[31]
$La_{0.20}Ca_{0.80}MnO_3$	bulk	o.21	[31]
$La_{0.10}Ca_{0.90}MnO_3$	bulk	0.63	[31]
$La_{0.05}Ca_{0.95}MnO_3$	bulk	0.004	[31]
$La_{0.375}Ca_{0.625}MnO_3$	Bulk	2.95	Present work
$La_{0.50}Ca_{0.50}MnO_3$	20 nm	0.09	[30]
$La_{0.33}Ca_{0.67}MnO_3$	20 nm	0.20	[30]
$La_{0.25}Ca_{0.75}MnO_3$	40 nm	0.38	[30]
$La_{0.375}Ca_{0.625}MnO_3$	200 nm	o.72	Present work
$Sm_{0.50}Ca_{0.50}MnO_3$	bulk	1.24	[17]
$Sm_{0.45}Ca_{0.55}MnO_3$	bulk	2.078	[17]
$Sm_{0.40}Ca_{0.60}MnO_3$	bulk	2.48	[17]
$Sm_{0.35}Ca_{0.65}MnO_3$	bulk	0.96	[17]
$Sm_{0.30}Ca_{0.70}MnO_3$	bulk	0.54	[17]
$Pr_{0.33}Ca_{0.67}MnO_3$	bulk	0.14	[6]

ordered (pnma) phase [25]. A. Martinelli et al. have suggested about the phase separation during cooling. The phase separation between Antiferromagnetic structure with canted spin ordering in ac plane (associated with charge-orbital ordered phase) and cy type spin arrangement (associated with disordered polymorph) may play a significant role for the existence of exchange bias effect. The existence of surface strain and atomic displacement influences the exchange anisotropy [6]. From structural point of view, this type of disorder can modify the interface exchange constant which is responsible for exchange bias effect.

Niebieskikwiat and Salamon have already reported that for phase separated manganite system, exchange bias field (H_E) depends on the

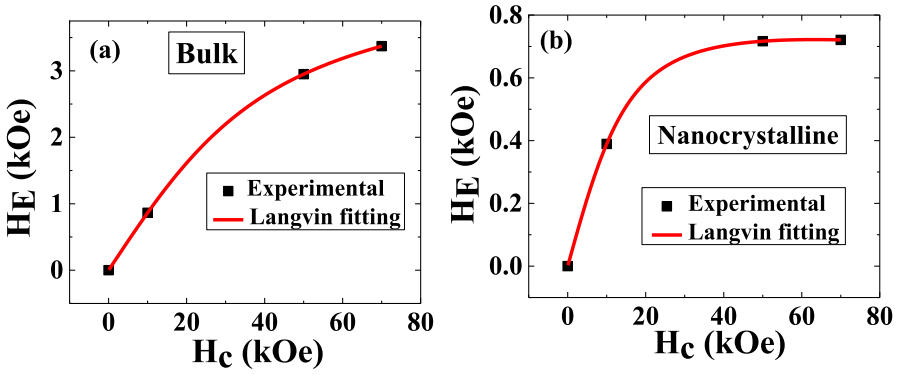

Fig. 5. (a) and (b) represents the variation of calculated exchange bias field with the cooling field for bulk and nanoparticles respectively. Red lines represent the fitting using Eq. (1) for both the compounds.

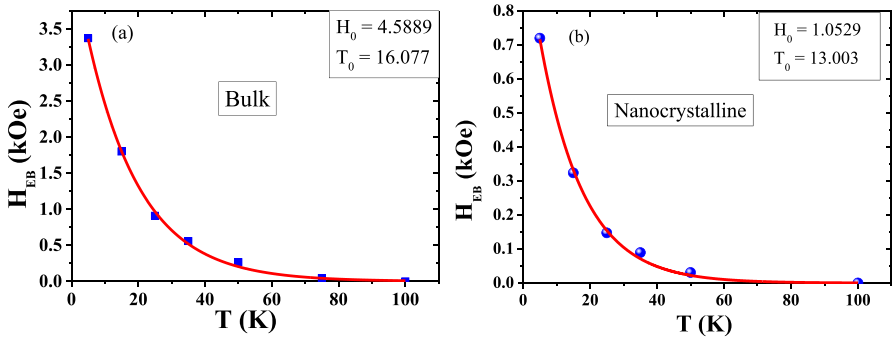

Fig. 6. (a) and (b) represents the variation of calculated exchange bias field (H_E) with temperature at H = 70kOe magnetic field for bulk and nanoparticles respectively.

cooling field (H_C) by the following relation

$$-H_E \propto J_i[\frac{J_i\mu_0}{(g\mu_B)^2} La(\frac{\mu H_C}{K_B T_f}) + H_C] \quad (2)$$

Where J_i is interfacial exchange constant, $\mu_0 = 3\mu_B$ (magnetic moment of Mn core spin where μ_B is bohr magneton), g~2 (gyromagnetic factor), $\mu = N_v\mu_0$ (magnetic moment of ferromagnetic clusters), La denotes the Langevin function, T_f is the temperature below which the glassy phase exists [6,32]. For smaller value of cooling field $H_E \propto J_i^2$ (first term dominates) and for large value of cooling field $H_E \propto J_i$ (second term is important). From Fig. 5 we have estimated the average number of spins in cluster (N_v) and average size of short-range ferromagnetic cluster by fitting the Niebieskikwiat and Salaman equation.

In Fig. 5(a) and (b) the scattered experimental data are well fitted with the model described above. In Eq. (3), Nv and J_i are the adjustable parameters. The exchange constant for bulk sample shows negative value ($J_i < 0$), whereas for nanocrystalline it gives positive value ($J_i > 0$). It is already reported that negative value ($J_i < 0$) indicates the presence of ferromagnetic clusters in the antiferromagnetic host and for high cooling field a tendency of the reduction of H_E may be observed [6,17]. The number of spins per ferromagnetic droplet (using Eq. (3)) for the bulk sample is $Nv \sim 8$ (taking $T_f \sim 25$ K) and for nanocrystalline (~200 nm) $Nv \sim 30$ (considering $T_f \sim 40$ K) which indicates larger ferromagnetic droplet diameter of the nanocrystalline sample compared to the bulk counterpart. With decreasing particle size ferromagnetic fraction increases, one can expect the exchange bias effect for $La_{0.375}Ca_{0.625}MnO_3$ nanoparticles also. But, here the suppression of charge order stability reduces the value of exchange bias effect. For the nano sized system, the presence of surface and size effect, pinning centers may lead to more complex behavior and they also play a significant role for the reduction of exchange bias value for nanoparticles in comparison to bulk counterpart.

The temperature dependence of the exchange bias effect (cooling field = 70 kOe) for the bulk and nanocrystalline compound is plotted in Fig. 6. The H_E vs. T curves are fitted by using the formula

$$H_E = H_0 exp(-\frac{T}{T_0}) \quad (3)$$

where T_0 and H_0 are fitting parameters [37]. In case of the both compound the magnitude of the exchange bias is sharply decreases with increasing temperature, similar as reported earlier [6,37].

4. Conclusions:

In summary, we have studied the magnetic and exchange bias effect of a very special type of the charge ordered compound (polycrystalline bulk and Nanocrystalline $La_{0.375}Ca_{0.625}MnO_3$ compound). Our experimental result indicates that Exchange bias effect for bulk compound is significantly large for both the charge order stability (large value of T_{CO}) and structural transition. The unidirectional spin pinning is greatly modified in the nanostructure sample with the modification of disordered polymorphic phase (exist in bulk compound) within the charge orbital ordered phase.

Declaration of competing interest

The authors declare that they have no known competing financial interests or personal relationships that could have appeared to influence the work reported in this paper.

Acknowledgments

The work was supported by Department of Atomic Energy (DAE), Govt. of India. We are grateful to S. Kumar, R. Mondal, and N. Mondal for FESEM measurement.

References

[1] A. Biswas, T. Samanta, S. Banerjee, I. Das, J. Appl. Phys. 103 (2008) 013912.
[2] A. Biswas, S. Chandra, T. Samanta, M.H. Phan, I. Das, H. Srikanth, J. Appl. Phys. 113 (2013) 17A902.
[3] N.S. Bingham, P. Lampen, M.H. Phan, T.D. Hoang, H.D. Chinh, C.L. Zhang, S. W.Cheong, H. Srikanth, Phys. Rev. B 86 (2012) 064420.
[4] P. Lampen, N.S. Bingham, M.H. Phan, H. Kim, M. Osofsky, A. Pique, T.L. Phan, S.C. Yu, H. Srikanth, Appl. Phys. Lett. 102 (2013) 062414.
[5] V.B. Shenoy, D.D. Sarma, C.N.R. Rao, Chem. Phys. Chem. 7 (2006) 2053–2059.
[6] D. Niebieskikwiat, M.B. Salamon, Phys. Rev. B 72 (2005) 174422(1)–174422(6).
[7] K. OGrady, L.E. Fernandez-Outon, G. Vallejo-Fernandez, J. Magn. Magn. Mater. 322 (2010) 883–899.
[8] A.E. Berkowitz, J.I. Hong, S.K. McCall, E. Shipton, K.T. Chan, T. Leo, D.J. Smith, Phys. Rev. B 81 (2010) 134404.
[9] A. Mannan, A. Patrick, H.M. Christopher, G. Denis, J. Bryan, L.S. Robert, Nature Mater. 6 (2007) 70–75.
[10] C. William, M.H. Kryder, J. Appl. Phys. 67 (1990) 5722–5724.
[11] Ch. Binek, S. Polisetty, X. He, A. Berger, Phys. Rev. Lett. 96 (2006) 067201.
[12] P.J. van der Zaag, R.M. Wolf, A.R. Ball, C. Bordel, L.F. Feiner, R. Jungblut, J. Magn. Magn. Mater. 148 (1995) 346–348.
[13] M. Kishimoto, T. Sueyoshi, J. Hirata, et al., J. Appl. Phys. 50 (1979) 450–452.
[14] R.K. Zheng, H. Liu, X.X. Zhang, et al., Appl. Phys. Lett. 85 (2004) 2589–2591.
[15] M.H. Phan, J. Alonso, H. Khurshid, P.L. Kelley, S. Chandra, K.S. Repa, Z. Nemati, R. Das, Ó. Iglesias, H. Srikanth, Nanomaterials 6 (2016) 221.
[16] E. Maniv, R.A. Murphy, S.C. Haley, S. Doyle, C. John, A. Maniv, S.K. Ramakrishna, Y.L. Tang, P. Ercius, R. Ramesh, A.P. Reyes, J.R. Long, J.G. Analytis, Nat. Phys. 17 (2021) 525.
[17] P. Dasgupta, K. Das, S. Pakhira, C. Mazumdar, S. Mukherjee, S. Mukherjee, A. Poddar, Sci. Rep. 7 (2017) 3220.
[18] U. Shankar, A.K. Singh, J. Phys. Chem. C 119 (2015) 28620.
[19] C.H. Patterson, Phys. Rev. B 72 (2005) 085125.
[20] P. Levy, F. Parisi, G. Polla, D. Vega, G. Leyva, H. Lanza, R.S. Freitas, L. Ghivelder, Phys. Rev. B 62 (2000) 6437.
[21] T. Sarkar, B. Ghosh, A.K. Raychaudhuri, T. Chatterji, Phys. Rev. B 77 (2008) 235112.
[22] J.L. Martínez, A. de Andrésa, M. García, Hernándeza, C. Prieto, J.M. Alonso, E. HerreroJ, González-Calbet, M. Vallet-Regí, J. Magn. Magn. Mater. 196-197 (1999) 520–521.
[23] S.W. Cheong, H.Y. Hwang, in: Y. Tokura (Ed.), Contribution to Colossal Magnetoresistance Oxides, Monographs in Condensed Matter Science, Gordon and Breach, London, 1999.
[24] C.L. Lu, S. Dong, K.F. Wang, F. Gao, P.L. Li, L.Y. Lv, J.-M. Liu, Appl. Phys. Lett. 91 (2007) 032502.
[25] A. Martinelli, M. Ferretti, C. Ritter, J. Solid State Chem. 239 (2016) 99–105.
[26] A. Biswas, I. Das, J. Appl. Phys. 102 (2007) 064303.
[27] A. Biswas, I. Das, C. Majumdar, J. Appl. Phys. 98 (2005) 124310.
[28] S. Dong, F. Gao, Z.Q. Wang, J.M. Liu, Z.F. Ren, Appl. Phys. Lett. 90 (2007) 082508.
[29] S. Dong, R. Yu, S. Yunoki, J.M. Liu, E. Dagotto, Phys. Rev. B 78 (2008) 064414.
[30] S.M. Zhou, S.Y. Zhao, Y.Q. Guo, J.Y. Zhao, L. Shi, J. Appl. Phys. 107 (2010) 033906.
[31] X.H. Huang, Z.L. Jiang, X.F. Sun, G. Xiao, J. Li, J. Am. Ceram. Soc. 94 (2011) 1324–1326.
[32] M.B. Salamon, P. Lin, S.H. Chun, Phys. Rev. Lett. 88 (2002) 197203.
[33] S. Guo, D.P. Young, R.T. Macaluso, D.A. Browne, N.L. Henderson, J.Y. Chan, L.L. Henry, J.F. DiTusa, Phys. Rev. Lett. 100 (2008) 017209.
[34] W.J. Jiang, X.Z. Zhou, G. Williams, Y. Mukovskii, K. Glazyrin, Phys. Rev. Lett. 99 (2007) 177203.
[35] J. Nogues, J. Sort, V. Langlais, V. Skumryev, S. Surinach, J.S. Munoz, M.D. Baro, Phys. Rep. 422 (2005) 65–117.
[36] J. Nogues, I.K. Schuller, J. Magn. Magn. Mater. 192 (1999) 203–232.
[37] S.K. Giri, S.M. Yusuf, M.D. Mukadam, T.K. Nath, J. Appl. Phys. 115 (2014) 093906.